Nanotribological investigation of polymer brushes with lithographically defined and systematically varying grafting densities

Zhenyu J. Zhang,[1,#] Mark Moxey,[1,§] Abdullah Alswieleh,[1,¶] Steven P. Armes,[1] Andrew L. Lewis,[2] Mark Geoghegan,[3] and Graham J. Leggett[1,*]

[1]Department of Chemistry, University of Sheffield, Brook Hill, Sheffield, S3 7HF, UK

[2]Biocompatibles UK Ltd., Chapman House, Farnham Business Park, Weydon Lane, Farnham, Surrey, GU9 8QL, UK and [3]Department of Physics and Astronomy, University of Sheffield, Sheffield S3 7RH, UK Present address: [#]School of Chemical Engineering, University of Birmingham, Edgbaston, Birmingham B15 2TT, U.K. [§]Institute of Materials Research & Engineering, #08-03, 2 Fusionopolis Way, Innovis, Singapore 138634 [¶]Department of Chemistry, College of Science, King Saud University, PO Box 2455, Riyadh 11451, Saudi Arabia *To whom correspondence should be addressed. Email: Graham.Leggett@sheffield.ac.uk

TITLE RUNNING HEAD Frictional properties of patterned polymer brushes

*To whom correspondence should be addressed. E-mail: Graham.Leggett@sheffield.ac.uk

ABSTRACT

Following controlled photodeprotection of a 2-nitrophenylpropyloxycarbonyl-protected (aminopropyl)triethoxysilane (NPPOC-APTES) film and subsequent derivatization with a bromoester-based initiator, poly(2-(methacryloyloxy)ethyl phosphorylcholine) (PMPC) brushes with

various grafting densities were grown from planar silicon substrates using atom transfer radical polymerization (ATRP). The grafting density correlated closely with the extent of deprotection of the NPPOC-APTES. The coefficient of friction for such PMPC brushes was measured by friction force microscopy (FFM) in water and found to be inversely proportional to the grafting density due to the osmotic pressure that resists deformation. Deprotection of NPPOC-APTES via near-field photolithography using a range of writing rates enabled the fabrication of neighbouring nanoscopic polymeric structures with dimensions ranging from 100 to 1000 nm. Slow writing rates enable complete deprotection to occur, hence polymer brushes are formed with comparable thicknesses to macroscopic brushes grown under same conditions. However, the extent of deprotection is reduced at higher writing rates, resulting in the concomitant reduction of the brush thickness. The coefficient of friction for such polymer brushes varied smoothly with brush height, with lower coefficients being obtained at slower writing rate (increasing initiator density) because the solvated brush layer confers greater lubricity. However, when ultra-sharp probes were used for nanotribological measurements, the coefficient of friction increased with brush thickness. Under such conditions, the radius of curvature of the tip is comparable to the mean spacing between brush chains, allowing the probe to penetrate the brush layer leading to a relatively large contact area.

INTRODUCTION

Polymer brushes consist of dense layers of surface-immobilized polymers and present a flexible and versatile means to control surface properties. Using surface-initiated atom transfer radical polymerization (ATRP), highly biocompatible stimulus-responsive homopolymer or copolymer brushes can be conveniently prepared with controlled thickness, composition and density.[1-2] Because of these attributes, polymer brushes have been used extensively as components in molecular assembly.[3] Recently, there has been substantial interest in the use of polymer brushes in micro- and nano-systems. Combining micro- or nano-lithography with polymer synthesis[4-9] provides a versatile platform for fabricating a range of devices, e.g. templates for protein or cell adhesion,[10-11] biosensors with single molecule sensitivity,[12-13] and optical components such as gratings.[14-15] The additional functionality conferred by polymer brushes enables various potential applications to be explored. For

example, electron beam lithography was used[7] to generate micro- and nanoscale patterns, followed by the construction of arrays of poly(*N*-isopropylacrylamide) (PNIPAAm) brush lines that are responsive to surrounding solvents. In a series of studies concerning nanopatterned polymer brushes,[16-18] the design principles and fabrication of stimuli-responsive nano-objects suitable for sensing and actuation applications were explored and demonstrated.

One effective approach to control the responsiveness of surface-immobilized polymer films is to manipulate the interfacial brush conformation. At low grafting densities, the isolated brush chains adopt a mushroom conformation. As the brush grafting density increases, the excluded volume interactions between neighbouring chains become sufficiently great that the chains extend well away from the surface to form a well-defined brush layer. Although the mushroom-to-brush transition has been studied extensively at the macroscopic scale, the growing interest in micro- and nano-structured surface-immobilized polymer brushes raises important new questions regarding the structure-property relationships for such systems.

Conventional characterization techniques for macroscopic (unpatterned) brushes such as ellipsometry are unsuitable for micro- and nano-structured brushes. Therefore, SPM-based techniques have been used extensively to characterize the morphology and structure of nanoscale brushes. Friction force microscopy (FFM), which is a variant of scanning probe microscopy (SPM), has been used successfully to examine the surface chemical composition and mechanical properties with spatial resolution at the nm scale.[19-20] During an FFM measurement, the SPM cantilever moves laterally across the surface and the frictional force between the tip and the surface is monitored. In a recent work, we demonstrated that FFM is highly sensitive to solvent-induced changes in the structure of a polymer brush, because the energy dissipation mechanisms for such lateral interactions are very sensitive to changes in the brush conformation.[21-22] Similar results have been reported by other research groups.[23-25] For example, Li and colleagues characterized the tribological properties of surface grown polyacrylamide films of various crosslinking density in a series of methanol/water mixtures where solvent quality is controlled, and found that the frictional response is directly related to solvent quality and the degree of crosslinking [24]

In the present work, photolithography has been used to construct patterned polymer brushes over a range of length scales that exhibit systematically varying brush grafting densities. As described in Scheme 1, a film of an aminosilane with a photo-removable protecting group, nitrophenylpropyloxycarbonyl-protected aminopropyltriethoxysilane (NPPOC-APTES) was first formed on a planar silicon substrate .[26] Exposure of this adsorbate to near-UV irradiation (λ_{max} = 325 nm) causes quantitative deprotection of the amine group, which may then be derivatized by reacting with 2-bromoisobutyryl bromide (BIBB). This yields regions covered by surface-immobilized bromine atoms which act as initiators for ATRP. The extent of deprotection varies with UV exposure,[26] hence the density of initiator sites should be controlled, in principle, simply by varying the UV irradiation time. Here we examine for the first time the possibility of integrating this approach with ATRP to control the brush density for various nanostructures. One important advantage of this photochemical approach is that it is compatible with the use of a near-field probe for patterning; this approach is known as scanning near-field photolithography (SNP) and enables convenient access to submicrometer length scales whereby the the brush density is organized spatially within nanostructures. SNP has been used to fabricate structures as small as 9 nm for various materials, including alkylthiolate monolayers on gold,[27] alkylphosphonates on titania and alumina,[28] and alkylsilanes on silica.[29] In the present study, a near-field probe was used to write structures consisting of surface-immobilized polymer brushes by patterning the deprotection of NPPOC-APTES surface sites. The exposure is inversely proportional to the rate of motion of the probe, so the brush density can be controlled simply by varying the writing rate. A zwitterionic 2-(methacryloyloxy)ethyl phosphorylcholine) (MPC) monomer was used to prepare the brushes, because it confers excellent lubricious properties,[30] remarkable biocompatibility,[31-32] and is responsive to subtle changes in solvation.[21, 33-34]
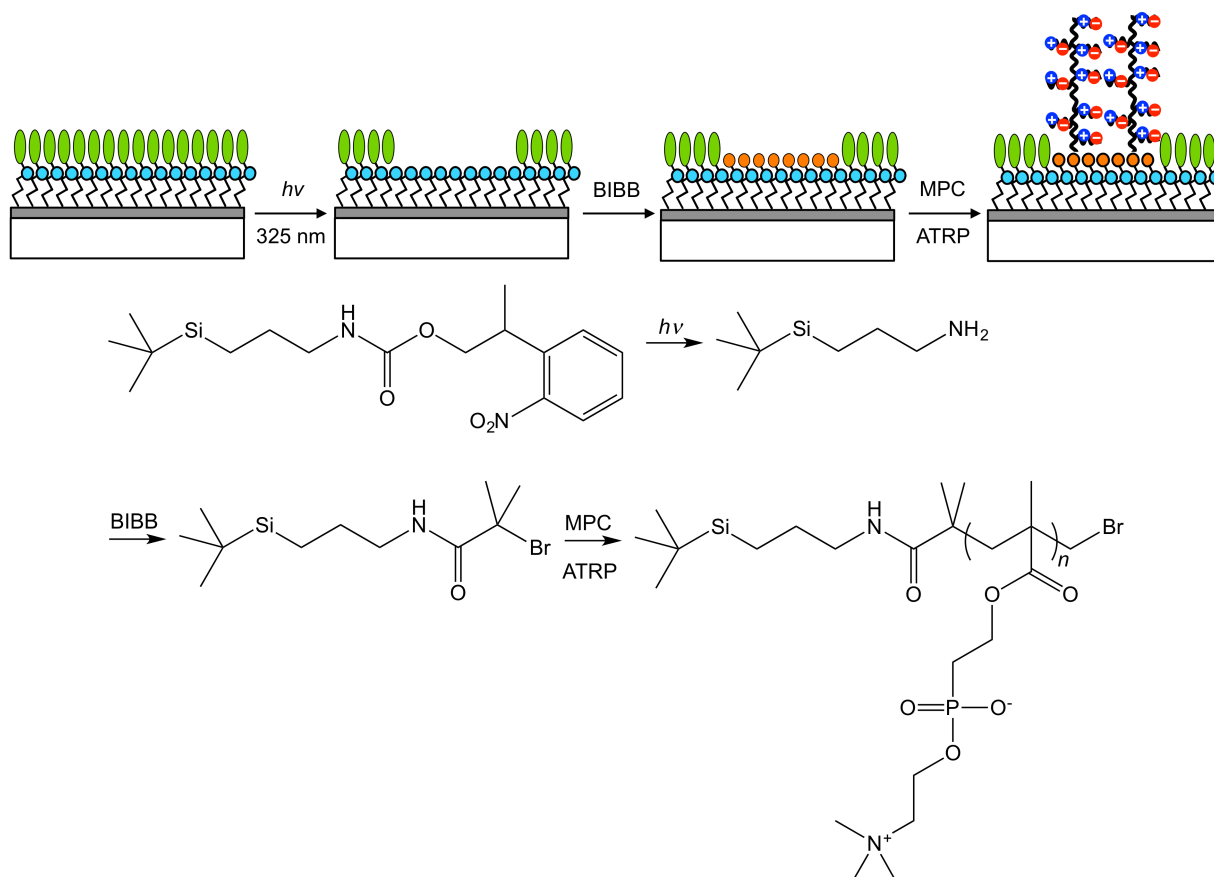
Scheme 1. Schematic diagram depicting: (a) exposure of a photolabile NPPOC-APTES surface layer to UV irradiation; (b) a patterned amine-functionalized film after NPPOC deprotection; (c) subsequent generation of initiator sites at the surface, and (d) surface-initiated ATRP of MPC.

EXPERIMENTAL

Materials

Triethylamine (TEA) (>99%), α-bromoisobutyryl bromide (BIBB) (98%), copper(I) bromide [Cu(I)Br, 99.999%], copper(II) bromide [Cu(II)Br$_2$, 99.999%], 2,2'-bipyridine (bpy, 99%) and ammonium hydroxide solution (28-30% NH$_3$ in H$_2$O) were purchased from Sigma-Aldrich (Dorset, UK). *N*-(2-(2-Nitrophenyl)propan-1-oxycarbonyl)-3-aminopropyl)triethoxysilane (NPPOC-APTES) films were synthesized as described previously.[26] 2-(Methacryloyloxy)ethyl phosphorylcholine monomer (MPC, > 99% purity) was kindly donated by Biocompatibles UK Ltd and was used as received. Sulfuric acid (1.83 S.G. 95+%), hydrogen peroxide solution (100 volumes 30+%), absolute ethanol (99.8+%), dichloromethane (DCM; HPLC grade) and toluene (HPLC grade) were supplied by Fisher Scientific (Loughborough, UK). Cover slips (22 mm x 64 mm No. 1.5) were supplied by Menzel-Gläser.

Preparation of silane films

All glassware used in the formation of films was first cleaned by immersion in piranha solution, which is a mixture of 30% hydrogen peroxide and 95% concentrated sulfuric acid in a 3:7 volume ratio, for at least 40 min. (*Caution: piranha solution is an extremely strong oxidising agent which has been known to detonate spontaneously upon contact with organic material*). All glassware was rinsed thoroughly with deionized water (Elga Pure Nanopore, 18.2 MΩ cm) at least six times and then sonicated for 10 min before drying overnight in an oven set at 80 °C.

Particular attention was paid to cleaning glass slides. Before immersion in piranha solution, slides were sonicated first in toluene, then in acetone, and finally in deionized water for 15 min. After treatment with piranha solution, slides were rinsed with deionized water and then immersed in RCA solution, a 1:1:5 (volume ratio) mixture of 30% hydrogen peroxide, ammonium hydroxide (28-30% NH_3 basis) and deionized water for 30 min. at 80 °C Slides were then rinsed thoroughly with deionized water before placing in an oven to dry at 80 °C.

Clean dried glass slides were subsequently immersed in a 1 mM solution of NPPOC-silane in toluene for 24 h. The treated slides were then rinsed in ethanol, sonicated in toluene and dried under a stream of dry nitrogen.

Photolithography and polymerization

Photodeprotection at the nm scale was conducted using an AlphaSNOM scanning near-field optical microscope (WiTec, Ulm, Germany), coupled with a He-Cd laser (IK3202R-D, Kimmon, Tokyo, Japan) operating at a wavelength of 325 nm. WiTec AlphaSNOM cantilever-type probes were used (WiTec, Ulm, Germany). Customized scripts were commissioned to translate the probe over the film at various rates (1 – 1000 μm/s). This protocol produces lines with various degrees of deprotection of the NPPOC groups. To fabricate micrometer-sized patterns, electron microscopy grids (Agar, Cambridge, UK) were used as a convenient mask at a laser power of 7.6 mW. NPPOC silane films were exposed to UV irradiation for 5 – 120 s (corresponding to doses in the range 0.2 – 4.7 J cm^{-2}) to produce various degrees of deprotection, which results in the formation of homogeneous brush layers with differing grafting densities.

After photolithography, the patterned planar substrates were placed under a nitrogen atmosphere using three pump-refill cycles of up to twelve Schlenk tubes in a Radley's Carousel 12 Plus Reaction Station. For the polymerization solution, MPC monomer, bipy, CuBr and $CuBr_2$ were used at a relative molar ratio of 60:2.8:1:0.3. Ultrapure deionized water was deoxygenated via a nitrogen purge for at least 30 min. MPC was weighed into a flask, which was then sealed and deoxygenated with dry nitrogen. Known masses of CuBr, $CuBr_2$ and bipy were then added to the flask. The deoxygenated water was added via syringe to produce an aqueous solution, which was sonicated for 15 min to aid dissolution. This reaction solution was then injected into the twelve Schlenk tubes, making sure to cover the planar substrates completely. MPC polymerization was terminated after 30 min by exposure to air, which oxidized the brown Cu(I) ATRP catalyst to form an inactive blue Cu(II) species. The PMPC brush-coated planar substrates were rinsed with methanol and ultrapure deionized water in turn and then sonicated for 5 min while immersed in a 1:1 acetone/water mixture, followed by drying under a stream of nitrogen gas.

Ellipsometry

A phase-modulated spectroscopic ellipsometer (M-2000V, J.A. Woollam Inc., USA) was used to measure the mean PMPC brush thickness. Samples were positioned in a measurement chamber filled with 15 mL ultrapure water. The refractive index for PMPC was estimated using the Cauchy parameters $A_n = 1.4778$ and $B_n = 0.004775 \ \mu m^2$, as obtained from a previous study.[33] The brush layer was modelled as a single slab of variable thickness using the completeEASE software package (J. A. Woollam Inc.). Due to its highly swollen nature in a good solvent, the refractive index of the brush layer is between that of the pure dry PMPC chains and that of the water, and is modeled using a linear effective medium approximation (EMA). The refractive index of water was approximated using Cauchy parameters of $A_n = 1.3242$ and $B_n = 0.003064 \ \mu m^2$.

Friction force microscopy

Friction force measurements were conducted using a Digital Instruments Multimode atomic force microscope equipped with a Nanoscope IV controller (Bruker, Cambridge, UK) operating in contact mode. The friction response was determined from friction loops acquired by obtaining forward-

reverse scan cycles with the microscope employed in scope mode. The friction signal was obtained by subtracting the mean signals in both directions, giving a resultant force that is twice the frictional force. The scan size was adjusted depending on the polymer brush width, while the scan rate was maintained at 1000 nm s^{-1}. A liquid cell fitted with a silicone O-ring was used for all measurements.

Two types of SPM cantilevers of differing tip radii (MLCT and SNL, Veeco, Cambridge, UK) were used. Unless specifically mentioned, MLCT cantilevers were used in this study. Cantilever spring constants were determined by recording their thermal spectra following the method developed by Hutter and Bechhoefer.[35] The lateral signal was converted from voltage to force by using the wedge method, in which the cantilever is scanned across a calibration grating (TGF11, MikroMasch, Tallinn, Estonia) and the friction signal is measured as a function of applied load.[36-37] The tip radius was characterized by translating the probe across a calibration grating (TGG01, Mikromash, Tallinn, Estonia) at scanning angles of 0° and 90°.

RESULTS and DISCUSSION

Effect of grafting density

To examine whether the brush grafting density can be controlled by photolithography, films formed by the adsorption of NPPOC-APTES on borosilicate substrates were exposed to UV irradiation followed by contact angle measurements, as shown in Figure 1a. The contact angle of the as-prepared film was 66 ± 2°, and a gradual reduction in contact angle was observed with exposure time, reaching a minimum value of 58.8 ± 0.4°. The photochemical deprotection of NPPOC-APTES films has been studied extensively,[26] showing that deprotection is quantitative after exposure at 325 nm leading to surfaces that exhibit identical reactivity to control surfaces formed by the adsorption of APTES. The contact angle changes observed here, and the rates of change, are consistent with the previous work.[26] In the present work, samples were categorized according to their UV dose, as determined by the output power of the UV source, the exposure time, and the area of illumination. While the change in contact angle is relatively modest, it is nevertheless significant compared to the experimental uncertainty, which enables the extent of surface modification to be conveniently monitored.

After UV irradiation, each planar surface was derivatized by reaction with BIBB to introduce surface initiator sites, followed by surface-initiated polymerization of MPC. Previous work on NPPOC-APTES[26] and related nitrophenyl protecting groups[38] has demonatrated that quantitative deprotection is achieved at full exposure, and that the reactivity of deprotected APTES is indistinguishable from that of control surfaces formed by the direct adsorption of APTES. A direct measurement of the brush molecular weight is not usually feasible for polymer chains grown from a planar substrate.[39] However, the volume fraction of polymer chains within the brush layer can be calculated from ellipsometric measurements. When a hydrophilic PMPC brush is exposed to a good solvent such as water, the swollen brush layer consists of both PMPC and solvent molecules, and its refractive index lies between that of the pure solvent and that of dry PMPC. Hence a linear effective medium approximation (EMA) model was used to interpret the ellipsometric data. The EMA model contains two variables: the thickness of the swollen brush layer d and the volume fraction of polymer chains in the swollen layer ψ. The mass of grafted polymer chains per unit surface area (Γ), is defined as[33]

$$\Gamma = \rho \int_{0}^{d} \varphi_p(z)dz, \qquad (1)$$

where ρ is the density (solid-state) of pure PMPC, ϕ_p is the polymer volume fraction which is dependent on the distance from the underlying surface, z is the distance from the surface. The equation can be simplied as

$$\Gamma = \rho d \psi \qquad (2)$$

because the density profile is presumed as constant in the single-slab model. The adsorbed mass of PMPC chains in the brush layer, normalized to that of the polymer layer grown from the fully deprotected film (after ~ 4.7 J cm^{-2} UV irradiation), is presented as a function of UV dose in Figure 1b. Clearly, there is a close correlation between the normalized mass of PMPC and the contact angle: both parameters change rapidly up to 1.6 J cm^{-2} and then more slowly, approaching a limiting value at a dose of between 3 and 5 J cm^{-2}. As the contact angle declines, the fraction of deprotected adsorbates (ie. The fraction of free amines available for reaction with BIBB) increases; the density

of initiators thus increases in proportion to the decrease in the contact angle. Hence, comparing the data in Figures 1a and b we can infer that the polymer chain density is proportional to the extent of deprotection of NPPOC-APTES. Controlled photodeprotection of NPPOC-APTES is thus an effective means of preparing polymer brushes of varying grafting density.

Frictional coefficients were determined for PMPC brushes immersed in water as a function of their surface grafting density, by measuring gradients from plots of the friction force against applied load. Figure 1c shows the variation in coefficient of friction with the UV dose. PMPC brushes exhibit substantial lubricity in a good solvent such as water.[21, 30] This is attributed to the osmotic pressure that results from binding of solvent molecules to such zwitterionic polymer chains.[40] This osmotic pressure resists deformation of the PMPC chains by the SPM tip, so that the energy dissipated in plowing friction is reduced. It has been estimated that there may be up to 25 water molecules associated with each PMPC monomer unit.[41-42] These water molecules prevent significant deformation of the extended PMPC chains, hence reducing the amount of energy dissipation under an applied load. The coefficient of friction is reduced as the UV dose is increased, because this leads to a higher surface density of amine groups, which results in a larger number of initiator sites being available for polymerization. As the surface density of PMPC chains increases, there is a corresponding increase in the osmotic pressure that resists brush deformation.
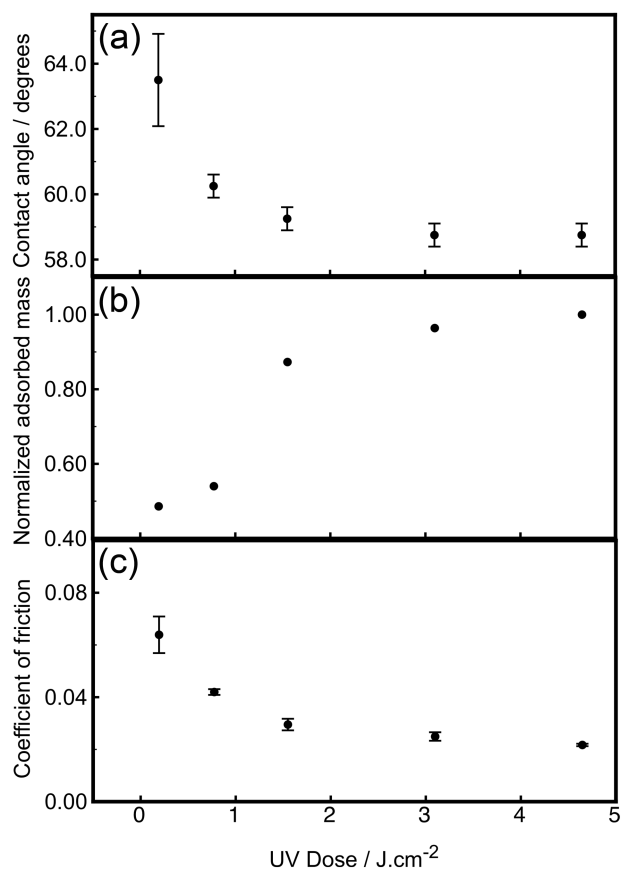
Figure 1. (a) Contact angle of NPPOC-protected silane film after UV irradiation; (b) ratio of adsorbed mass of PMPC brush to that of the brush grown from the fully deprotected monolayer; (c) coefficients of friction determined for homogeneous PMPC brush layers immersed in water as a function of the UV irradiation dose. The adsorbed mass indicates the PMPC brush grafting density.

There is an initial rapid reduction in the coefficient of friction (μ) for UV doses of up to 1.6 J cm^{-2}, but thereafter μ decreased more slowly, reaching a limiting value of 0.020 at between 3 and 5 J cm^{-2}, which is consistent with the observed change in the normalized brush volume fraction of PMPC in a swollen brush. The correlation between the variation in coefficient of friction and the contact angle with UV dose is striking, suggesting that the brush density is directly related to the surface amine concentration obtained after deprotection: at the highest UV doses, the NPPOC surface groups are extensively deprotected and an extended brush structure is most likely formed on exposure to water. The data shown in Figure 1 indicates a relatively decrease change in the coefficient of friction as the density of grafted polymers increases.

Micropatterned brushes

To produce patterned PMPC brushes on the μm scale, NPPOC-protected silane films were irradiated using a mask, followed by the same surface ATRP protocol as that used to prepare homogeneous (unpatterned) PMPC brushes. Figure 2a shows a SPM height image of a

11

representative sample. A cross-sectional analysis of the patterned brush layer, corresponding to the black line in Figure 2a, is presented in Figure 2b. Quantitative friction measurements were conducted on at least five 1×1 μm^2 squares for each sample. The mean coefficient of friction acquired at the centres of these squares was 0.020 ± 0.001, which is in good agreement with the coefficient determined for the unpatterned PMPC brush layer grown from the fully deprotected silane film. This suggests that the brush grafting density is comparable in each case.
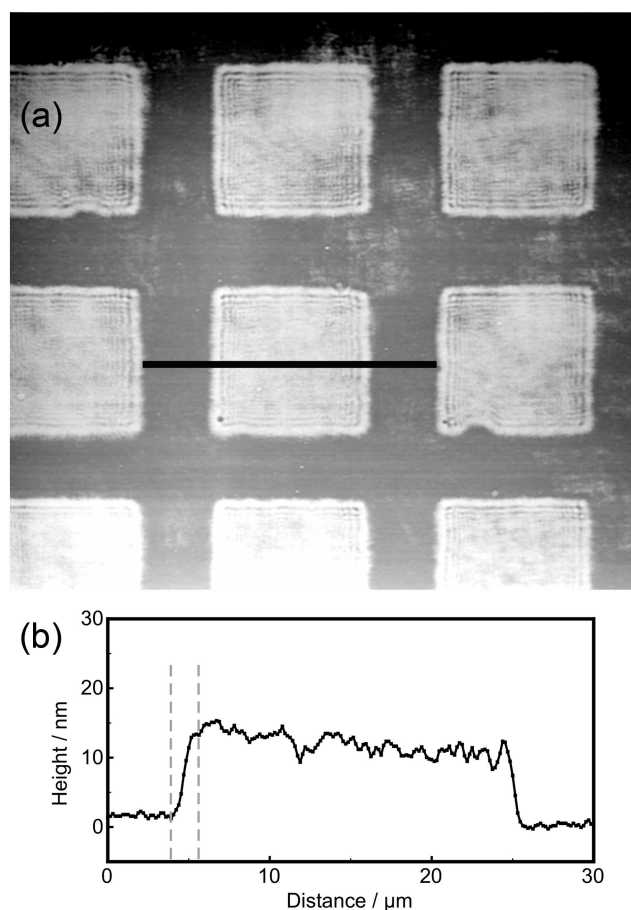
Figure 2. (a) SPM height image of a micropatterned PMPC brush layer in water; (b) cross-section analysis corresponds to the black line. The observed height variation between the two gray dashed lines is caused by the difference in PMPC brush grafting density.

Nanopatterned brushes

Nanometer-scale patterns were fabricated on NPPOC-protected silane films using scanning near-field photolithography. A cantilever-based scanning near-field optical microscope (SNOM) probe was used that had a hollow square pyramidal tip with an aperture at its apex. The probe was traced across the sample surface, causing UV photodeprotection of NPPOC-APTES to generate a series of lines. The scan frequency was maintained at a constant value, and the length of the line traced by the probe was increased monotonically. After polymer growth by ATRP, the sample was imaged using

SPM (Figure 3a shows a representative SPM image). A total of 15 lines were generated: the line length was increased, while maintaining a fixed scan *frequency*, leading to a progressive increase in the scan *speed*. The tip speed followed the sequence 10, 20, 40, 60, 80, 100, 125, 150, 175, 200, 250, 300, 400, 500, and 1000 nm s^{-1} from left to the right to generate the desired pattern. The laser pathway was blocked temporarily before the probe returned to the origin (marked by the arrow) to confirm that deprotection was achieved by photochemical removal of the protecting group, rather than by physical contact (scratching) of the SNOM probe. It is worth noting that both micro- and nanopatterned samples were prepared with the same polymerization time and in the same reaction vial to ensure consistencywhich warrants a direct comparison between the two sets of brushes.

The mean feature width is progressively reduced from left to right in Figure 3a. This is because, as the line length increases, there is a concomitant increase in the scan rate that effectively controls the UV exposure time (e.g. doubling the scan rate halves the probe dwell time at each point along the feature). Thus the extent of UV exposure is reduced as the scan rate is increased, leading to deprotection of a smaller fraction of the NPPOC groups. Consequently, a less densely-grafted brush was formed vis surface-initiated ATRP. The reduced contrast from left to right in Figure 4a reflects progressively lower heights, indicating that a systematic reduction in initiator site density leads to a lower brush grafting density, as expected.

Figure 3b shows the the mean exposure used for each feature, based on the aperture size, laser input power, and SNOM tip velocity, where it intersects the black line drawn in Figure 3a. Figure 3c shows the variation in height along the black line: there is a gradual reduction in feature height that correlates closely with the reduction in UV exposure indicated in Figure 3b. Finally, each brush line was then imaged individually and its height was determined at more than ten locations. Mean heights for each line are shown in Figure 3d, with line widths ranging from 1000 nm (for the shortest line) to 100 nm. Clearly, the heights indicated in Figure 3d correlate closely with those depicted in Figure 3c. The tallest features have similar heights to those of the micropatterned brush shown in Figure 2. This suggests that the tallest lines comprise brush-like chains, which is the case for the majority of the microstructures shown in Figure 2. As the scan rate is increased, the brush height is

smoothly reduced. This suggests a smooth continuum in behavior at lower grafting densities, rather than an abrupt brush-to-mushroom transition.
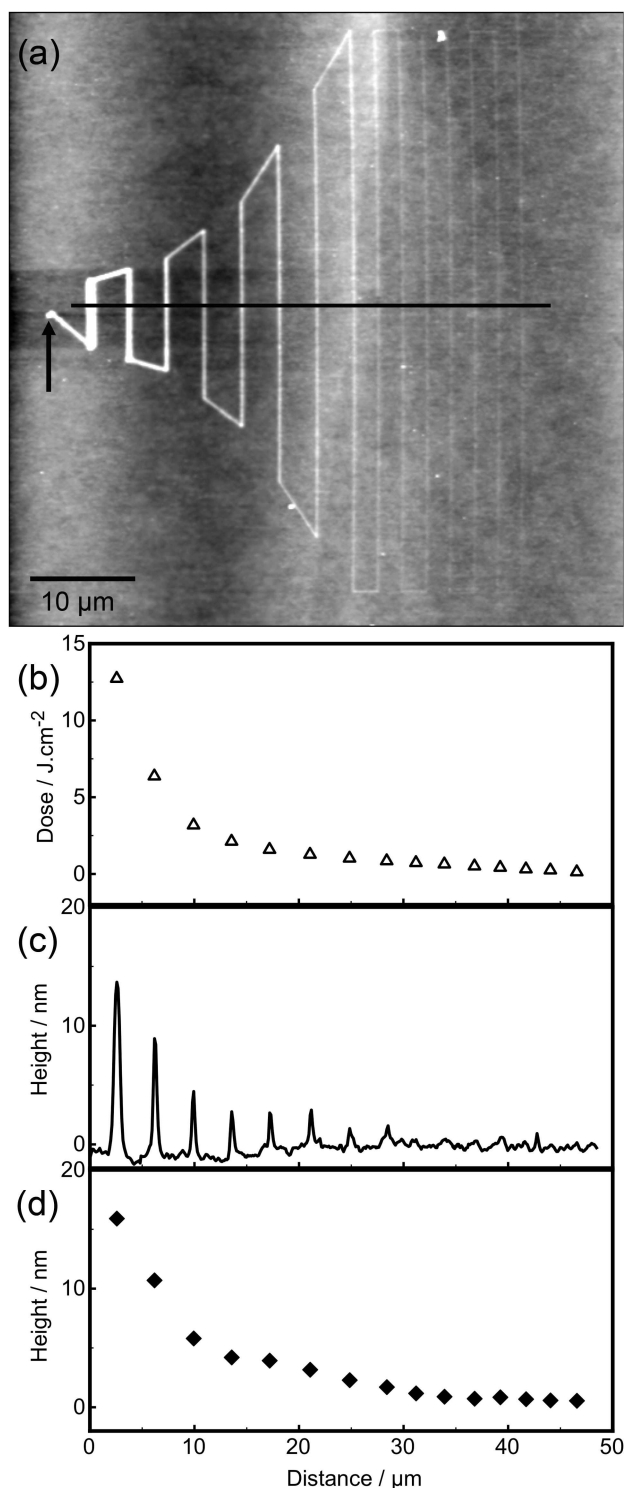
Figure 3. (a) SPM height image obtained for a nanopatterned PMPC brush acquired in water (arrow indicates the starting position of the SNOM probe); (b) calculated UV irradiation dose; (c) cross-section analysis corresponds to the black line; (d) mean height averaged over at least ten locations; as a function of the relative distance of each brush line. Error bars are not shown but are similar in magnitude to the dimensions of the symbols used in the graph.
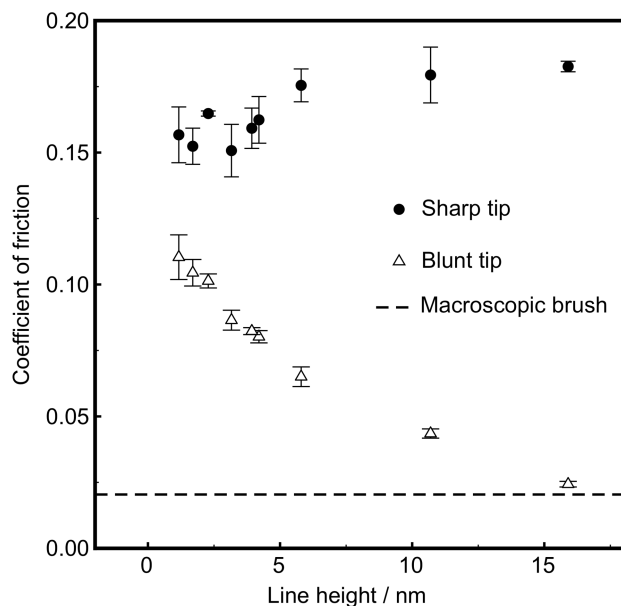
Figure 4. Mean coefficients of friction as a function of PMPC brush height, acquired using a sharp tip (SNL cantilever) or a blunt tip (MLCT cantilever). The dashed line corresponds to the mean coefficient of friction determined for a macroscopic PMPC brush. Error bars correspond to the standard error values for the experimental results.

Friction measurements were conducted in water. In this solvent, PMPC chains are highly hydrated, which favors a brush-like conformation.[33] To examine how the contact area between an SPM probe and the PMPC brush affects the friction measurement, SPM cantilevers of varying tip radius were utilized. The tip radii of SNL and MLCT cantilevers are 9.7 ± 0.5 and 56 ± 5 nm, respectively, as determined by moving each probe along a calibration grid. Figure 4 shows the coefficients of friction acquired as a function of brush height and brush grafting density, with the latter parameter increasing from left to right. When a larger tip is used, a lower coefficient of friction is observed at higher brush grafting densities, which is consistent with the well-known highly lubricious nature of PMPC brushes.[30, 43] For a brush thickness of 16 nm, the coefficient of friction is very similar to that measured for the microstructured polymer brush shown in Figure 2. This is consistent with the above suggestion that the grafted PMPC chains adopt a brush conformation for the tallest nanolines. At lower grafting densities (feature heights), the coefficient of friction is reduced. It is also noteworthy that there is a smooth relationship between the coefficient of friction and the feature height: there is no sharp transition from the brush (16 nm height) to the mushroom (2 nm height) regime. This gradual evolution is consistent with the brush height data.

The deformation energy of a molten polymer brush has been studied,[44] and it was found that the force required to produce local deformation using a blunt AFM tip depends on the tip radius (R), the mean degree of polymerization of the brush (ε), and the brush height (h_0) by

$$F \approx -\frac{192\varepsilon^3 R^2 \mu_0}{\pi^2 h_0^3}$$
. (3)

In contrast with the FFM data obtained using a blunt probe, a slight increase in the coefficient of friction was observed for taller lines when using a sharp tip. This is because the brush contact area is reduced for a sharp probe, so the number of chains within the contact area is reduced; the probe penetrates between adjacent chains and the lubricious effect of the highly hydrated chains is lost. Only when the contact area is larger (ie where the contact area comprises multiple chains) does the effect of the higher osmotic pressure become significant.

Previous studies by various groups[21, 33-34, 43] have shown that a 90/10 v/v ethanol/water mixture is a non-solvent for PMPC. In this environment, the dehydrated chains adopt a collapsed conformation, leading to a substantial reduction in the brush thickness. Moreover, FFM measurements on PMPC brush layers in various solvents confirmed that the coefficient of friction is directly related to the conformation of PMPC chains.[21] Figure 5 shows data obtained for the first four (widest) brush lines acquired when immersed in a 90/10 v/v ethanol/water mixture. In contrast to the brush behavior observed in pure water, the coefficient of friction depends less strongly on the brush grafting density in this solvent mixture. This is because the tip is able to deform desolvated PMPC chains much more readily, thus providing a wide range of energy dissipation pathways via chain deformation and enhanced plowing. Such solvent-responsive behavior could be a key factor in nanofabrication, e.g. for regulating fluid flow.[45-46]
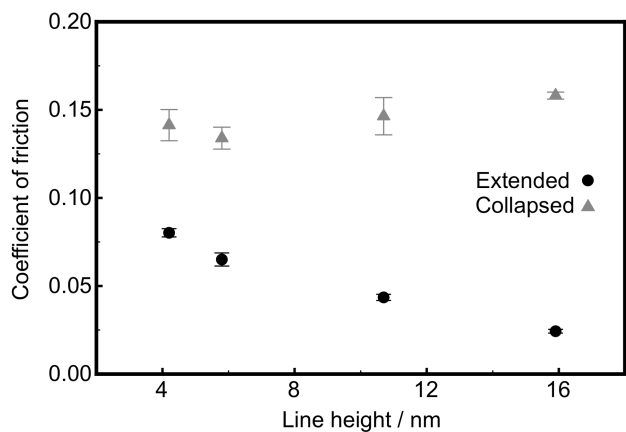
Figure 5. Coefficients of friction acquired on the first four PMPC lines when immersed in water (which produces highly extended brushes), or in a 90/10 v/v ethanol/water mixture (which produces collapsed brushes).

CONCLUSIONS

Deprotection of nitrophenyl-functionalized silane films on both unpatterned and patterned planar substrates has been achieved. Subsequently, surface-initiated ATRP of MPC was performed to construct a library of biocompatible brushes of variable grafting densities. The efficacy of near-field lithography for the fabrication of nanopatterned brushes using a photodeprotection strategy based on selective UV irradiation has been demonstrated. The mechanical properties of the resulting brushes were examined on different length scales. Nanostructured brushes behave similarly to conventional brushes, with the former system also offering unique potential for nanofabrication.

The quantitative correlation between coefficient of friction measured and height of nanopatterned feature demonstrates that friction force microscopy could be a unique approach to examine polymer brushes with nm-scale spatial arrangement. Furthermore, frictional properties of polymer brushes would be another means to reflect the conformational change of polymeric chains in liquid environment.

REFERENCES

1.   Edmondson, S.; Osborne, V. L.; Huck, W. T. S. Polymer brushes *via* surface-initiated polymerizations. *Chem. Soc. Rev.,* **2004,** *33*, 14-22.

2.   Zhao, B.; Brittain, W. J. Polymer brushes: surface-immobilized macromolecules. *Prog. Polym. Sci.,* **2000,** *25,* 677-710.

3.   Bünsow, J.; Kelby, T. S.; Huck, W. T. S. Polymer Brushes: Routes toward Mechanosensitive Surfaces. *Acc. Chem. Res.,* **2010,** *43,* 466-474.

4.   Rastogi, A.; Paik, M. Y.; Tanaka, M.; Ober, C. K. Direct Patterning of Intrinsically Electron Beam Sensitive Polymer Brushes. *ACS Nano,* **2010,** *4,* 771-780.

5.   Pernites, R. B.; Foster, E. L.; Felipe, M. J. L.; Robinson, M.; Advincula, R. C. Patterned Surfaces Combining Polymer Brushes and Conducting Polymer via Colloidal Template Electropolymerization. *Adv. Mater.,* **2011,** *23,* 1287-1292.

6.   Zhou, X.; Wang, X.; Shen, Y.; Xie, Z.; Zheng, Z. Fabrication of Arbitrary Three-Dimensional Polymer Structures by Rational Control of the Spacing between Nanobrushes. *Angew. Chem. Int. Ed.,* **2011,** *50,* 6506-6510.

7.   Kaholek, M.; Lee, W.-K.; Feng, J.; LaMattina, B.; Dyer, D. J.; Zauscher, S. Weak Polyelectrolyte Brush Arrays Fabricated by Combining Electron-Beam Lithography with Surface-Initiated Photopolymerization. *Chem. Mater.,* **2006,** *18,* 3660-3664.

8.   Ahmad, S. A.; Hucknall, A.; Chilkoti, A.; Leggett, G. J. Protein Patterning by UV-Induced Photodegradation of Poly(oligo(ethylene glycol) methacrylate) Brushes. *Langmuir,* **2010,** *26,* 9937-9942.

9.   Ducker, R.; Garcia, A.; Zhang, J.; Chen, T.; Zauscher, S. Polymeric and Biomacromolecular Brush Nanostructures: Progress in Synthesis, Patterning and Characterization. *Soft Matter,* **2008,** *4,* 1774-1786.

10.   Harris, B. P.; Kutty, J. K.; Fritz, E. W.; Webb, C. K.; Burg, K. J. L.; Metters, A. T. Photopatterned Polymer Brushes Promoting Cell Adhesion Gradients. *Langmuir,* **2006,** *22,* 4467-4471.

11.   Ahmad, S. A. A.; Wong, L. S.; ul-Haq, E.; Hobbs, J. K.; Leggett, G. J.; Micklefield, J. Protein Micro- and Nanopatterning Using Aminosilanes with Protein-Resistant Photolabile Protecting Groups. *J. Am. Chem. Soc.,* **2011,** *133,* 2749-2759.

12.   Senaratne, W.; Andruzzi, L.; Ober, C. K. Self-Assembled Monolayers and Polymer Brushes in Biotechnology: Current Applications and Future Perspectives. *Biomacromolecules,* **2005,** *6,* 2427-2448.

13.   Salazar, R. B.; Shovsky, A.; Schönherr, H.; Vancso, G. J. Dip-Pen Nanolithography on (Bio)Reactive Monolayer and Block-Copolymer Platforms: Deposition of Lines of Single Macromolecules. *Small,* **2006,** *2,* 1274-1282.

14.   Valkama, S.; Kosonen, H.; Ruokolainen, J.; Haatainen, T.; Torkkeli, M.; Serimaa, R.; Brinke, T. G.; Ikkala, O. Self-Assembled Polymeric Solid Films with Temperature-Induced Large and Reversible Photonic-Bandgap Switching. *Nat. Mater.,* **2004,** *3,* 872-876.

15.   Campbell, M.; Sharp, D. N.; Harrison, M. T.; Denning, R. G.; Turberfield, A. J. Fabrication of Photonic Crystals for the Visible Spectrum by Holographic Lithography. *Nature,* **2000,** *404,* 53-56.

16.   Patra, M.; Linse, P. Simulation of grafted polymers on nanopatterned surfaces. *Nano Lett.,* **2006,** *6,* 133-137.

17.   Paik, M. Y.; Xu, Y.; Rastogi, A.; Tanaka, M.; Yi, Y.; Ober, C. K. Patterning of polymer brushes. A direct approach to complex, sub-surface structures. *Nano Lett.,* **2010,** *10,* 3873-3879.

18.   Zhou, F.; Biesheuvel, M.; Choi, E.-Y.; Shu, W.; Poetes, R.; Steiner, U.; Huck, W. T. S. Polyelectrolyte brush amplified electroactuation of microcantilevers. *Nano Lett.,* **2008,** *8,* 725-730.

19.   Leggett, G. J.; Brewer, N. J.; Chong, K. S. L. Friction Force Microscopy: Towards Quantitative Analysis of Molecular Organisation with Nanometre Spatial Resolution. *Phys. Chem. Chem. Phys.,* **2005,** *7,* 1107-1120.

20.   Bhushan, B., *Nanotribology and Nanomechanics: An Introduction.* 2nd ed.; Springer: 2008.

21.   Zhang, Z.; Morse, A. J.; Armes, S. P.; Lewis, A. L.; Geoghegan, M.; Leggett, G. J. Effect of Brush Thickness and Solvent Composition on the Friction Force Response of Poly(2-(methacryloyloxy)ethylphosphorylcholine) Brushes. *Langmuir,* **2011,** 2514-2521.

22.   Zhang, Z.; Moxey, M.; Ablswieleh, A.; Morse, A. J.; Lewis, A. L.; Geoghegan, M.; Leggett, G. J. Effect of salt on phosphorylcholine-based zwitterionic polymer brushes. *Langmuir,* **2016**, 5048-5057.

23.   Perry, S. S.; Yan, X.; Limpoco, F. T.; Lee, S.; Müller, M.; Spencer, N. D. Tribological Properties of Poly(l-lysine)-graft-poly(ethylene glycol) Films: Influence of Polymer Architecture and Adsorbed Conformation. *ACS Appl. Mater. Interfaces,* **2009**, *1*, 1224-1230.

24.   Li, A.; Ramakrishna, S. N.; Kooij, E. S.; Espinosa-Marzal, R. M.; Spencer, N. D. Poly(acrylamide) Films at the Solvent-Induced Glass Transition: Adhesion, Tribology, and the Influence of Crosslinking. *Soft Matter,* **2012**, *8*, 9092-9100.

25.   Nordgren, N.; Rutland, M. W. Tunable Nanolubrication between Dual-Responsive Polyionic Grafts. *Nano Lett.,* **2009**, *9*, 2984-2990.

26.   Ahmad, S. A. A.; Wong, L. S.; ul-Haq, E.; Hobbs, J. K.; Leggett, G. J.; Micklefield, J. Micrometer- and Nanometer-Scale Photopatterning Using 2-Nitrophenylpropyloxycarbonyl-Protected Aminosiloxane Monolayers. *J. Am. Chem. Soc.,* **2009**, *131*, 1513-1522.

27.   Ducker, R.; Leggett, G. J. A mild etch for the fabrication of three-dimensional nanostructures in gold. *J. Am. Chem. Soc.,* **2006**, *128*, 392-393.

28.   Tizazu, G.; Adawi, A. M.; Leggett, G. J.; Lidzey, D. G. Photopatterning, etching, and derivatization of self-assembled monolayers of phosphonic acids on the native oxide of titanium. *Langmuir,* **2009**, *25*, 10746-10753.

29.   Sun, S.; Montague, M.; Critchley, K.; Chen, M.-S.; Dressick, W. J.; Evans, S. D.; Leggett, G. J. Fabrication of biological nanostructures by scanning near-field photolithography of chloromethylphenylsioxane monolayers. *Nano Lett.,* **2006**, *6*, 29-33.

30.   Chen, M.; Briscoe, W. H.; Armes, S. P.; Klein, J. Lubrication at Physiological Pressures by Polyzwitterionic Brushes. *Science,* **2009**, *323*, 1698-1701.

31.   Ma, I. Y.; Lobb, E. J.; Billingham, N. C.; Armes, S. P.; Lewis, A. L.; Lloyd, A. W.; Salvage, J. Synthesis of Biocompatible Polymers. 1. Homopolymerization of 2-Methacryloyloxyethyl Phosphorylcholine via ATRP in Protic Solvents: An Optimization Study. *Macromolecules,* **2002**, *35*, 9306-9314.

32.   Iwasaki, Y.; Ishihara, K. Phosphorylcholine-containing polymers for biomedical applications. *Anal. Bioanal. Chem.,* **2005**, *381*, 534-546.

33.   Edmondson, S.; Nguyen, N. T.; Lewis, A. L.; Armes, S. P. Co-Nonsolvency Effects for Surface-Initiated Poly(2-(methacryloyloxy)ethyl phosphorylcholine) Brushes in Alcohol/Water Mixtures. *Langmuir,* **2010**, *26*, 7216-7226.

34.   Kiritoshi, Y.; Ishihara, K. Molecular Recognition of Alcohol by Volume Phase Transition of Cross-linked Poly (2-methacryloyloxyethyl phosphorylcholine) Gel. *Sci. Tech. Adv. Mater.,* **2003**, *4*, 93-98.

35.   Hutter, J. L.; Bechhoefer, J. Calibration of Atomic-Force Microscope Tips. *Rev. Sci. Instrum.,* **1993**, *64*, 1868-1873.

36.   Ogletree, D. F.; Carpick, R. W.; and Salmeron, M. Calibration of Frictional Forces in Atomic Force Microscopy. *Rev. Sci. Instrum.,* **1996**, *67*, 3298-3306.

37.   Varenberg, M.; Etsion, I.; Halperin, G. An Impoved Wedge Calibration Method for Lateral Force in Atomic Force Microscopy. *Rev. Sci. Instrum.,* **2003**, *74*, 3362-3367.

38.   Xia, S.; Cartron, M.; Morby, J.; Bryant, D. A.; Hunter, C. N.; Leggett, G. J. Fabrication of Nanometer- and Micrometer-Scale Protein Structures by Site-Specific Immobilization of Histidine-Tagged Proteins to Aminosiloxane Films with Photoremovable Protein-Resistant Protecting Groups. *Langmuir,* **2016**, *32*, 1818-1827.

39.   Turgman-Cohen, S.; Genzer, J. Simultaneous bulk- and surface-initiated controlled radical polymerization from planar substrates. *J. Am. Chem. Soc.,* **2011**, *133*, 17567-17569.

40.   Kitano, H.; Sudo, K.; Ichikawa, K.; Ide, M.; Ishihara, K. Raman Spectroscopic Study on the Structure of Water in Aqueous Polyelectrolyte Solutions. *J. Phys. Chem. B,* **2000**, *104*, 11425-11429.

41.   Ishihara, K.; Nomura, H.; Mihara, T.; Kurita, K.; Iwasaki, Y.; Nakabayashi, N. Why Do Phospholipid Polymers Reduce Protein Adsorption? *J. Biomed. Mater. Res.,* **1998**, *39*, 323-330.

42.   Yaseen, M.; Lu, J. R.; Webster, J. R. P.; Penfold, J. The Structure of Zwitterionic Phosphocholine Surfactant Monolayers. *Langmuir,* **2006,** *22*, 5825-5832.

43.   Kobayashi, M.; Terayama, Y.; Hosaka, N.; Kaido, M.; Suzuki, A.; Yamada, N.; Torikai, N.; Ishihara, K.; Takahara, A. Friction Behavior of High-density Poly(2-methacryloyloxyethyl phosphorylcholine) Brush in Aqueous Media. *Soft Matter,* **2007,** *3*, 740-746.

44.   Fredrickson, G. H.; Ajdari, A.; Leibler, L.; Carton, J. P. Surface modes and deformation energy of a molten polymer brush. *Macromolecules,* **1992,** *25*, 2882.

45.   Beebe, D. J.; Moore, J. S.; Bauer, J. M.; Yu, Q.; Liu, R. H.; Devadoss, C.; Jo, B.-H. Functional Hydrogel Structures for Autonomous Flow Control Inside Microfluidic Channels. *Nature,* **2000,** *406*, 588-590.

46.   Gil, E.; Hudson, S. M. Stimuli-Responsive Polymers and Their Bioconjugates. *Prog. Polym. Sci.,* **2004,** *29*, 1173-1222.